AGU PUBLICATIONS

JGR

Journal of Geophysical Research: Space Physics

RESEARCH ARTICLE

10.1002/2016JA022491

Key Points:

- A sunrise enhancement in the vertical drift over Jicamarca
- Uplifted h_mF_2, decreased f_oF_2, and F_3 layer during the sunrise enhancement drift
- The first time to observe and simulate the effects of the sunrise enhancement drift on the ionosphere

Correspondence to:
L. Liu,
liul@mail.iggcas.ac.cn

Citation:
Zhang, R., L. Liu, H. Le, and Y. Chen (2016), Evidence and effects of the sunrise enhancement of the equatorial vertical plasma drift in the *F* region ionosphere, *J. Geophys. Res. Space Physics*, *121*, 4826–4834, doi:10.1002/2016JA022491.

Received 5 FEB 2016
Accepted 5 MAY 2016
Accepted article online 13 MAY 2016
Published online 26 MAY 2016

Evidence and effects of the sunrise enhancement of the equatorial vertical plasma drift in the *F* region ionosphere

Ruilong Zhang[1,2,3], Libo Liu[1,2], Huijun Le[1,2], and Yiding Chen[1,2]

[1]Key Laboratory of Earth and Planetary Physics, Institute of Geology and Geophysics, Chinese Academy of Sciences, Beijing, China, [2]Beijing National Observatory of Space Environment, Institute of Geology and Geophysics, Chinese Academy of Sciences, Beijing, China, [3]University of the Chinese Academy of Sciences, Beijing, China

Abstract Recent studies based on the satellite observations demonstrated that the equatorial vertical plasma drift can also enhance near sunrise in a way similar to the prereversal enhancement. However, it is not clear whether the signature of this sunrise enhancement appears in observations with other sounding techniques. In this work, we explore the Jicamarca (12°S, 283.2°E) incoherent scatter radar measurements to present the evidence of sunrise enhancement in vertical plasma drift on 12 May and 10 June 2004, which are under magnetically quiet and solar minimum conditions. The effects of the sunrise enhancement on the ionosphere are, for the first time, investigated by analyzing the ionograms recorded by the Digisonde Portable Sounder at Jicamarca and conducting the Theoretical Ionospheric Model of the Earth in Institute of Geology and Geophysics, Chinese Academy of Sciences. The observations showed that, during the sunrise enhancement, the F_2 layer peak height is lifted remarkably, and the F_2 layer peak density and bottomside electron density tend to decrease compared to the days without sunrise enhancements. The simulations indicated that the sunrise enhancement drift can lift the equatorial ionosphere to higher heights and distort the equatorial electron density profiles. What is more, the simulations display an F_3 layer in the equatorial *F* region during the sunrise enhancement, and a new F_2 layer develops at lower altitudes under the jointed control of the usual photochemical and dynamical processes.

1. Introduction

The equatorial *F* region vertical plasma drift can play important roles in the variations of equatorial ionospheric plasma density and composition and further affect the generation and evolution of plasma structures such as the equatorial ionization anomaly [e.g., *Bittencourt and Abdu*, 1981; *Basu et al.*, 2004, 2009; *Mannucci et al.*, 2005; *Abdu et al.*, 2008], equatorial irregularities [*Fejer et al.*, 1999], and F_3 layers [e.g., *Sen*, 1949; *Balan and Bailey*, 1995; *Balan et al.*, 1997, 1998, 2000; *Zhao et al.*, 2011a, 2011b; *Klimenko et al.*, 2012].

Extensive research with incoherent scatter radar (ISR), satellites, ionosondes, and models to investigate the equatorial *F* region vertical plasma drift has revealed that the vertical drift is generally upward in the daytime and downward in the nighttime during magnetically quiet times [e.g., *Fejer et al.*, 1991; *Fesen et al.*, 2000; *Kil et al.*, 2009; *Adebesin et al.*, 2013]. Also, it is characterized by enhancement near the sunset before its downward reversal, which is also known as the prereversal enhancement, PRE.

Recent studies based on the satellite observations presented something new near sunrise in the equatorial *F* region vertical plasma drift. The new feature is that the vertical plasma drift can also enhance near sunrise in a way similar to the PRE. For example, *Aggson et al.* [1995] and *Kelley et al.* [2014] reported some cases of sunrise enhancement in the variability of equatorial *F* region vertical plasma drift from the San Marco Satellite and the Communication/Navigation Outage Forecasting System satellite, respectively. Subsequently, *Zhang et al.* [2015] statistically investigated the occurrence of the sunrise enhancement using the measurements of the Republic of China Satellite-1. They reported that the sunrise enhancement occurrence has the seasonal and longitudinal variations that were most frequent during June solstice and in regions with the positive declination.

Up to now, the sunrise enhancement drift phenomenon is not well understood. The sunrise enhancements in vertical drifts reported in the above works are all from the satellite observations. We still do not survey whether the sunrise enhancement phenomenon can be detected from the observations with other techniques, such as the ISR and ionosondes. Interestingly, the signature of the sunrise enhancement is obvious on some days in the daily curves of the vertical plasma drift over Jicamarca (12°S, 283.2°E) in *Woodman* [1970]. It is better to provide evidence from further observations. Furthermore, what is the response of the ionosphere during the sunrise enhancement phenomenon? Unfortunately, no answer is found in previous reports.

In the current study, we explore the vertical drifts measured by the Jicamarca ISR to present the sunrise enhancement phenomenon on 12 May and 10 June 2004. The ionograms recorded by the Digisonde Portable Sounder (DPS) at Jicamarca are used to analyze the effects of the equatorial ionosphere during the cases of the sunrise enhancements registered by the Jicamarca ISR. The effects are further validated with the simulations by using the Theoretical Ionospheric Model of the Earth in Institute of Geology and Geophysics, Chinese Academy of Sciences [*Yue et al.*, 2008]. The results have key contributions to improve our understanding of equatorial ionospheric dynamics and structures near sunrise.

2. Data and Simulations

The *F* region vertical drifts were retrieved from the Jicamarca ISR. Many publications have excellently described the ISR sounding technique of the plasma drifts [e.g., *Fejer et al.*, 1991; *Kudeki et al.*, 1999]. Generally, the Jicamarca ISR observes plasma drifts at a resolution of 5 min in time and 15 km in height from about 200 to 600 km during low solar activity conditions. The vertical drift measurement errors are about 1–2 m/s during the day and become larger at high heights and late nights [*Fejer et al.*, 1991].

Currently, we used the vertical drift measurements at an altitude range from 200 to 450 km on 11 May, 12 May, and 10 June 2004. The measurement errors of the vertical drifts are smaller than 2 m/s. The observations are under low solar activity and geomagnetic quiet times. The values of solar index $F_{10.7}$ are 92 sfu (1 sfu = 10^{-22} Wm^{-2} Hz^{-1}) on 11 May, 100.9 sfu on 12 May, and 85 sfu on 10 June, and the daily geomagnetic *Ap* index reaches 12 nT on 11 May, 12 nT on 12 May, and 10 nT on 10 June, respectively. The interplanetary magnetic field (IMF) *Bz* component is not significantly deviated from zero on the three days, illustrating that the ionospheric vertical drifts are not severely affected by the processes of solar wind origin.

We also manually scaled the DPS ionograms recorded at Jicamarca and retrieved parameters of f_oF_2 (the critical frequency of the F_2 layer) and h_mF_2 (the peak height of the F_2 layer). Since f_oF_2 is directly related to N_mF_2 (the peak density of the F_2 layer), we use both without distinction in the following sectors. The SAO-Explorer true height inversion algorithm can derive the bottomside electron density profiles and reasonably extrapolate to altitudes above h_mF_2 to provide a whole profile using the method of *Huang and Reinisch* [2001]. These ionogram-derived electron density profiles are also used in the current study.

The model used in the present study is the Theoretical Ionospheric Model of the Earth in Institute of Geology and Geophysics, Chinese Academy of Sciences (TIME-IGGCAS). The TIME-IGGCAS model provides the plasma concentrations by solving the coupled equations of the momentum, energy, and mass continuity [*Yue et al.*, 2008]. The TIME-IGGCAS model required neutral compositions, and neutral winds are provided by the NRLMSIS-00 model (Mass Spectrometer and Incoherent Scatter) [*Picone et al.*, 2002] and the Horizontal Wind Model-93 [*Hedin et al.*, 1996]. The effect of the photoelectron heat adopts the method of *Millward* [1993]. The photoelectron heat comes from local sources at altitudes below 300 km. At altitudes above 300 km, the photoelectron heat is produced by both local sources and conjugated hemisphere sources.

3. Results

Figure 1 shows the combined observations from the ISR and DPS over Jicamarca on 10 June 2004. Figure 1 (top) presents the *F* region vertical plasma drifts over Jicamarca. The green points denote the vertical drifts observed with the ISR at altitudes from 200 to 450 km, and the red lines with dots represent the corresponding 15 min height-averaged vertical drifts. There is a data gap due to measurement interruption.

The blue line in Figure 1 (top) gives the vertical drifts on 10 June 2004 predicted from the empirical vertical drift model (S-F model) [*Scherliess and Fejer*, 1999]. The S-F model was built based on the drift observations from the Jicamarca ISR and the Atmospheric Explorer E satellite. Thus, the drifts predicted here by the S-F model can be considered to represent a climatologic characteristic at Jicamarca. We use the S-F model drift as a reference without sunrise enhancement under low solar activity and geomagnetic quiet times.

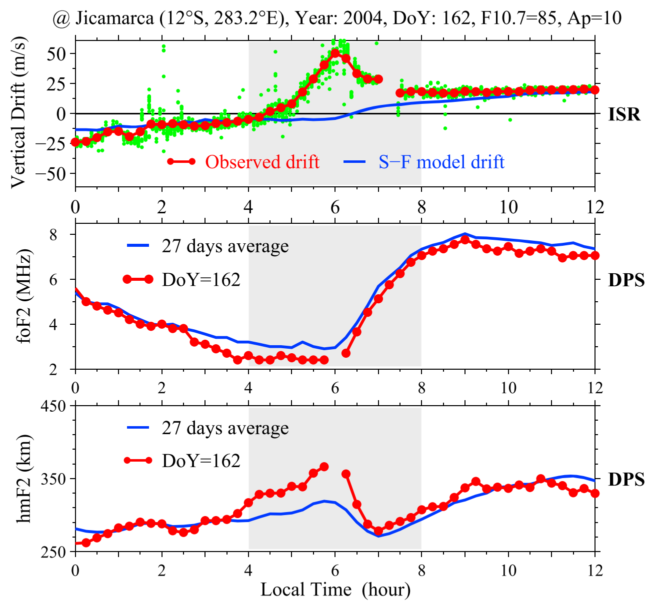

Figure 1. (top) The *F* region vertical plasma drifts at Jicamarca (12°S, 283.2°E) on 10 June 2004. The green points denote the vertical drifts observed with the incoherent scatter radar at heights from 200 km to 450 km, and the red line with dots represents the moving 15 min height-averaged values. The S-F model-predicted drifts are plotted with blue line as a reference. The daily values of $F_{10.7}$ and *Ap* indices are also marked. (middle and bottom) The red lines with dots exhibit the ionosonde f_oF_2 and h_mF_2 at Jicamarca on 10 June 2004. The corresponding 27 days average patterns are displayed with blue lines as a reference. The gray areas between 04:00 and 08:00 LT show the periods with a sunrise enhancement in vertical drifts.

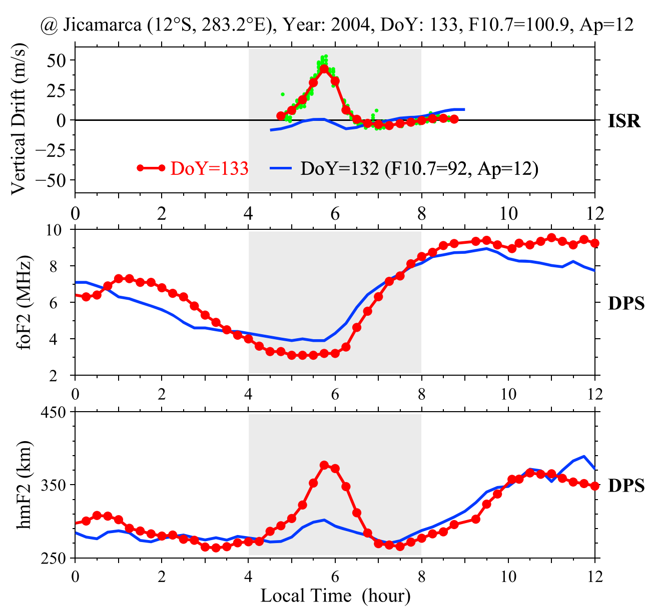

Figure 2. Same as Figure 1 but for another case on 12 May 2004. The data on 11 May 2004 are plotted with blue curves as a reference.

The ISR observations display an outstanding sunrise enhancement phenomenon in the vertical drifts on 10 June 2004. The enhancement has a peak magnitude as large as about 50 m/s. The vertical plasma drifts sharply decrease to normal levels at later hours after the sunrise peak. Moreover, as indicated from the extent of the scatter of points, there are somewhat altitude gradients in the vertical drifts during the sunrise enhancement.

Figure 1 (middle and bottom) plots the f_oF_2 and h_mF_2 recorded by the DPS over Jicamarca. The red lines with dots exhibit the observed values on 10 June 2004, and the blue lines represent 27 days average values. The gap results from a poor ionogram at 06:00 LT on 10 June. The blue lines display that the average f_oF_2 has a decrease tendency and the average h_mF_2 increases at the interval from 00:00 to 05:45 LT. As illustrated with the shaded area, h_mF_2 distinctly deviates from the 27 days average pattern, with a much stronger peak around 06 LT, and the f_oF_2 has a weak decrease compared to the 27 days average values. The huge deviation of h_mF_2 from the average values indicates the strong influence of the sunrise enhancement in vertical drifts observed by the ISR.

Figure 2 gives another case for the evidence and effects of the sunrise enhancement in the vertical drift on 12 May 2004 (red lines with dots). Figure 2 (top to bottom) displays the *F* region vertical plasma drifts, f_oF_2, and h_mF_2 over Jicamarca, respectively. The data on 11 May 2004 (blue lines) are plotted as a reference without sunrise enhancements. The green points in Figure 2 (top) present the observed drifts at altitudes from 200 to 450 km on 12 May 2004. There are abundant drift data gaps due to measurement interruptions.

As illustrated in Figure 2 (top), there is a drastically sunrise enhancement in the vertical drifts on 12 May 2004. The vertical drift is dramatically increased in magnitude and peaks at 05:45 LT with the magnitude of about 40 m/s. However, the 11 May 2004 observations display a very weak enhancement phenomenon

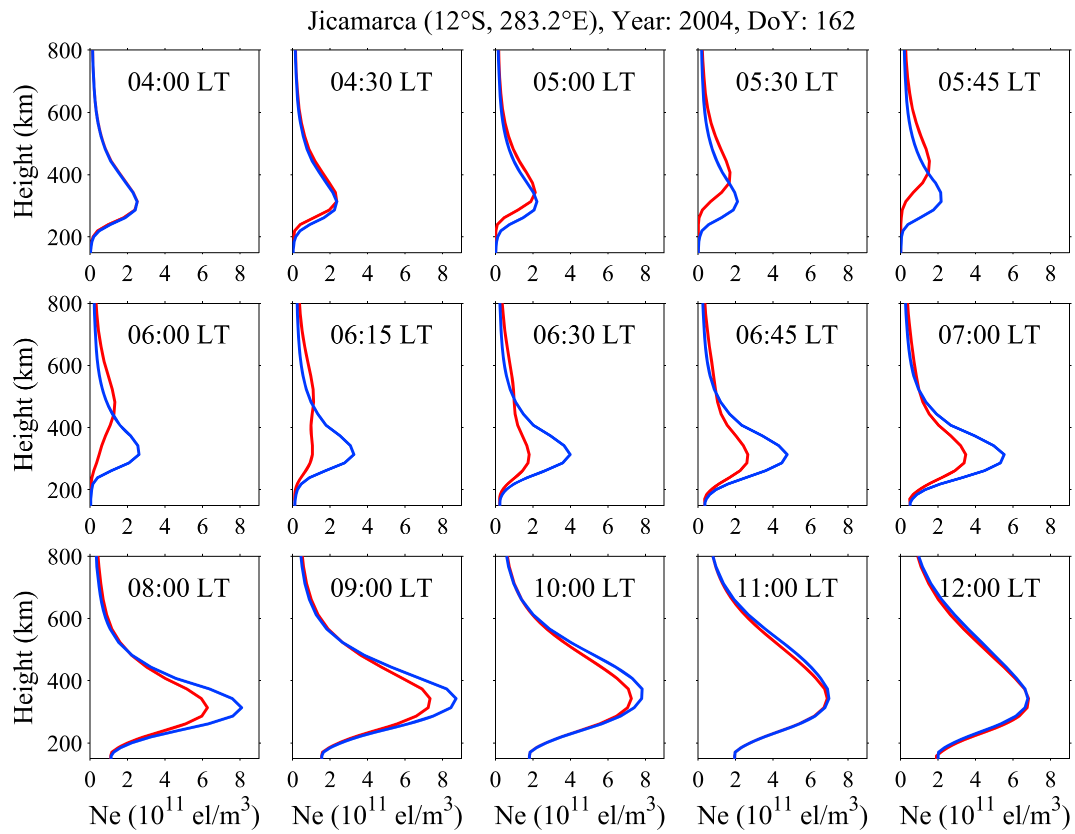

Figure 3. The electron density profiles calculated by the TIME-IGGCAS model with vertical drifts observed with the Jicamarca incoherent scatter radar on 10 June 2004 (red lines, sunrise enhancement case) and from the S-F model drifts (blue lines, no sunrise enhancement case).

in the vertical drifts, which can be considered as a day without sunrise enhancement. Thus, we use the values on 11 May as a reference of comparison. Figure 2 (middle and bottom) indicated that, when the enhancement presents in vertical drift near sunrise, there is an evident uplift in h_mF_2 and decrease in f_oF_2 compared to that on 11 May 2004.

To verify and further investigate the effects of the sunrise enhancement in the vertical drift on the ionosphere, we conducted a comparison of model simulations with two sets of the vertical drifts. The first run of the simulations uses the drifts calculated from the S-F model [*Scherliess and Fejer*, 1999] under the condition of 10 June 2004, and the second one uses the height-averaged drifts on 10 June 2004. In the two sets of simulations, we made no adjustment to the remaining input parameters of the model. It should be noted that there are some slight differences between the two cases of drifts before 04:00 LT on 10 June. These slight differences in the vertical drifts used for simulations, to some extent, will cause somewhat discrepancies in the model results near sunrise. Thereby, to remove such possible discrepancies, we use the S-F model drifts to replace the observed drifts at time before 04:00 LT in the second model run; namely, two cases of vertical drifts input in the simulations are taken the same ones before 04:00 LT.

Figure 3 shows some selected electron density profiles at Jicamarca on 10 June 2004 calculated with the TIME-IGGCAS model at the two cases, i.e., with the S-F model drifts (blue lines) and the observed drifts (red lines). The local times are labeled in the panels.

As can be seen from Figure 3, the sunrise enhancement drifts can drive distinct changes in the equatorial electron density profiles. Compared to the blue profiles (the conditions without sunrise enhancements), the peak heights of the red profiles are gradually moving toward higher altitudes, while the peak density tends to decrease. At altitudes above the peak height of the red profiles, the electron density is higher than those of the blue ones, while in the bottomside of the blue ones, the second run case has lower density.

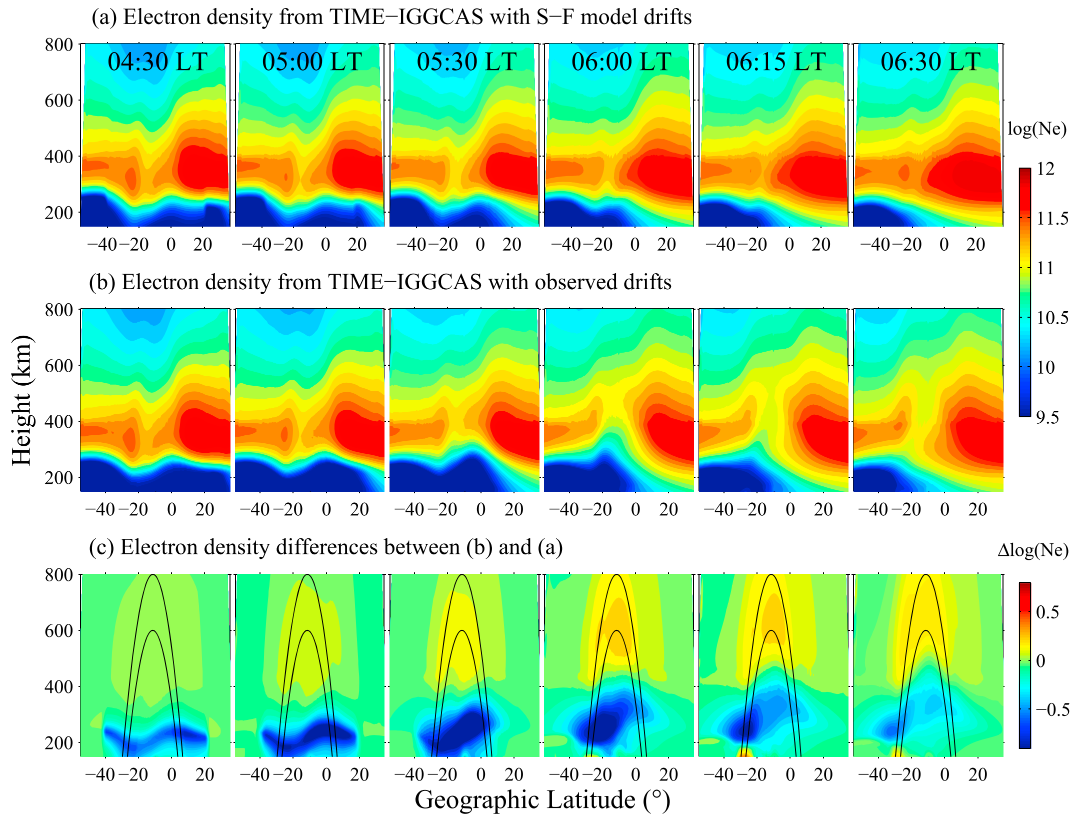

Figure 4. The electron density as a function of latitude and height from 04:30 to 06:30 LT on 10 June 2004, from TIME-IGGCAS simulations driven by (a) the S-F model drifts and (b) the observed drifts. (c) The electron density differences illustrated in Figures 4b and 4a. The black lines denote the geomagnetic field lines with peak heights of 600 km and 800 km in the magnetic equatorial plane.

Another fascinating feature in Figure 3 is the appearance of F_3 layer in simulations of the second run (the observed drifts case). At 06:15 LT, the F_2 layer is lifted to about 480 km. A new F_2 layer is formed at lower altitudes under the jointed control of the usual photochemical and dynamical processes. As a result, there are two peaks in the *F* region profiles; in other words, the upper peak is similar to the previously reported F_3 layers [*Balan and Bailey*, 1995]. As the time goes, the peak density of the new F_2 layer continuously increases and that of the F_3 layer rapidly decreases. Near about 06:30 LT, the F_2 layer peak density exceeds that of the F_3 layer, and the peak density of the F_3 layer is very small. After 06:45 LT, the F_3 layer disappears and the profiles recover to behave in the single *F* peak shape.

Figure 4 shows the electron density as a function of latitude and height from 04:30 LT to 06:30 LT on 10 June 2004, from the two runs of TIME-IGGCAS simulations with vertical drifts of (a) the S-F model and (b) Jicamarca ISR observations. Figure 4c displays the electron density differences at six snapshots illustrated in Figures 4b and 4a. Positive (negative) values in Figure 4c indicated that the electron density increases (reduces) under the influence of the sunrise enhancement drifts. The black lines denote the geomagnetic field lines with peak heights of 600 km and 800 km in the equatorial plane. Figure 5 exhibits the results at times from 07:00 to 12:00 LT in the similar style of Figure 4.

One can see from Figure 4a that a high-density region is first seen before 08:00 LT at about 20° latitude away from the magnetic equator in the Northern Hemisphere, which is understood as the effect of earlier sunrise in the Northern Hemisphere during June solstice. After that, another electron density crest region forms in the Southern Hemisphere, as demonstrated in Figure 5a.

Figure 4c indicates that the electron densities decrease in the bottomside and increase in the topside ionosphere associated with the sunrise enhancement drifts. The induced differences in electron density become most evident at 06:00 LT when the drift reaches its peak during the sunrise enhancement. The differences

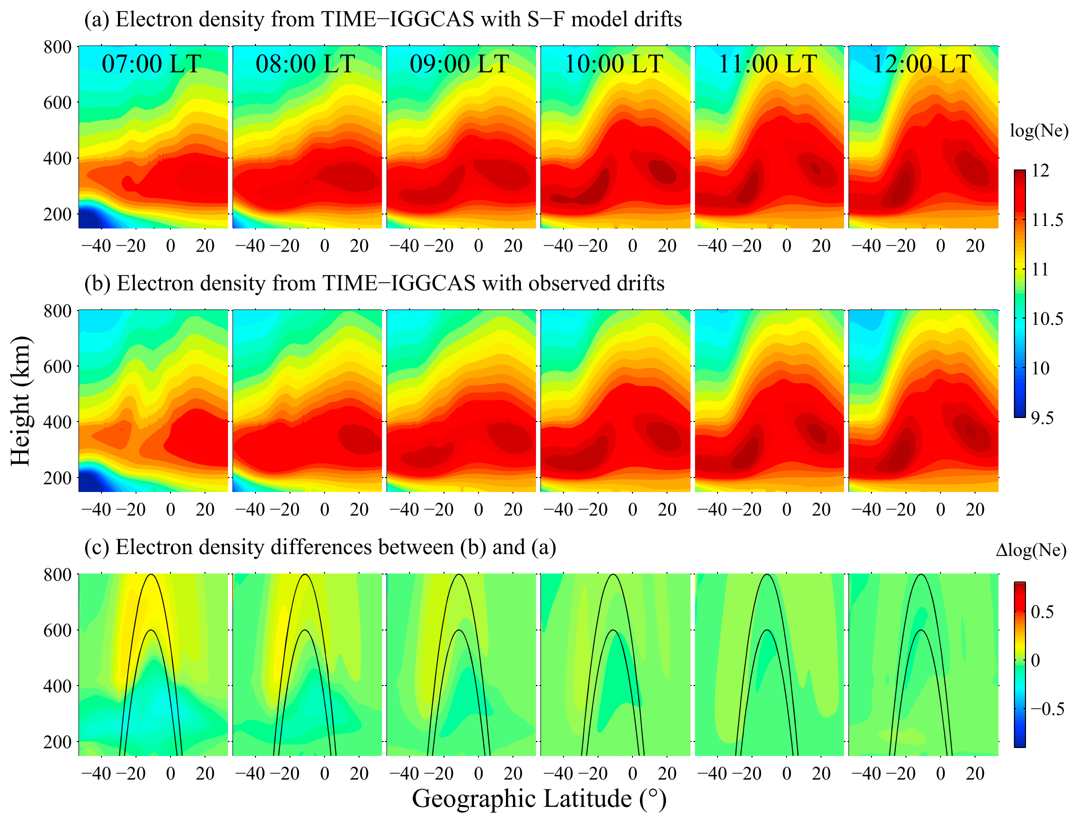

Figure 5. Same as Figure 4 but for later times (from 07:00 to 12:00 LT).

gradually diminish when two sets of vertical drifts are nearly similar with each other at 12:00 LT. These suggest that the dominating sunrise enhancement drifts can drive the equatorial ionosphere upward to higher altitudes compared to the conditions without sunrise enhancements.

The differences in electron density in Figure 4c reach a maximum at altitudes from about 600 km to 800 km, indicating that the sunrise enhancement drifts can drive the plasma upward at least up to about 800 km altitudes near sunrise in the equatorial ionosphere. Subsequently, at 800 km altitudes the lifted plasma will diffuse downward to both sides of the magnetic equator along the geomagnetic field lines due to the off-equator pressure gradient and gravity, which is generally known as equatorial plasma fountain effect [*Hanson and Moffett*, 1966]. After 06:15 LT, the transported plasma along the geomagnetic field lines has some asymmetries with the larger plasma flow in the Southern Hemisphere comparable to the Northern Hemisphere. This is because in June solstice circumstance, the trans-equatorial neutral winds can drag the plasma along the geomagnetic field lines from the Northern to Southern Hemisphere. With the enhanced equatorial plasma fountain during the sunrise enhancement, the locations of the crests are shifted to farther higher latitudes, which can be seen from Figures 4b and 5b.

4. Discussion

Among the simulated results, the most interesting feature is the formation of equatorial F_3 layer associated with the sunrise enhancement in the vertical drifts. The F_3 layer formation here is produced by the upward vertical drifts, which is similar with the one proposed earlier in *Balan and Bailey* [1995]. However, both the formation and maintenance of the F_3 layer are quite different in our simulations and those in *Balan and Bailey* [1995]. Such discrepancies are attributed to the different patterns of vertical drifts used in the simulations.

Unfortunately, the F_3 layer is not observed in the ionograms in the cases on 12 May and 10 June 2004. The ground-based DPS can only detect the bottomside ionosphere below the peak density, so in the ionograms the F_3 layer can be seen only when the peak density of the F_3 layer is greater than that of the F_2 layer. In

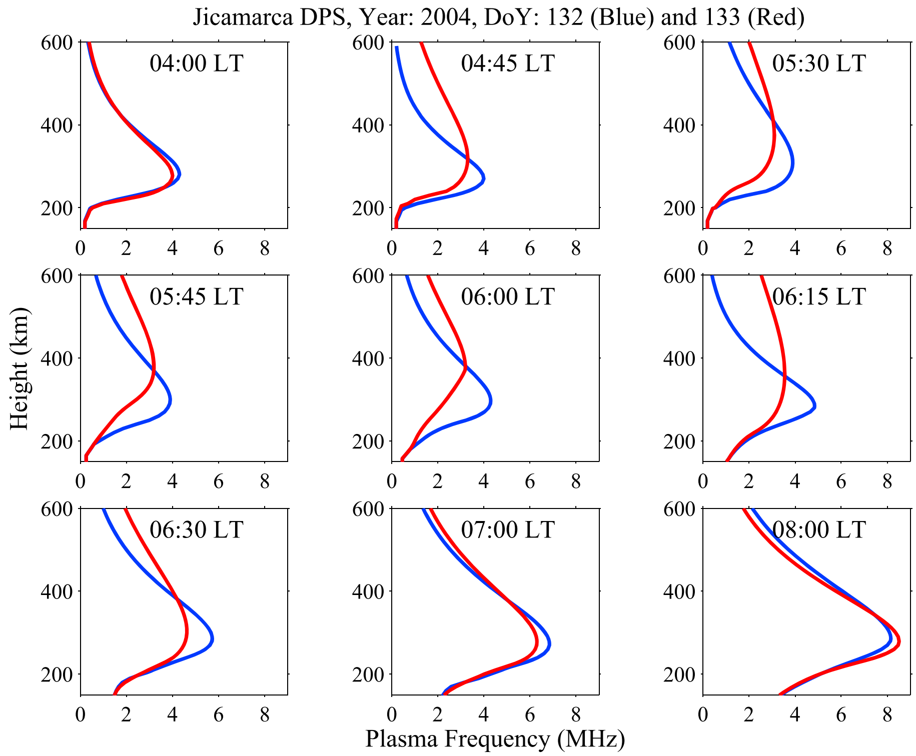

Figure 6. The ionogram-derived electron density profiles measured at Jicamarca on 11 (blue lines, no sunrise enhancement case) and 12 (red lines, sunrise enhancement case) May 2004.

current cases, although the F_3 layer is not directly appeared in the ionograms, some signatures hint its possible existence.

Figure 6 displays the ionogram-derived electron density profiles measured over Jicamarca on 11 (blue lines) and 12 (red lines) May 2004. The variation of the ionogram-derived profiles on 10 June 2004 is similar to that on 12 May 2004, we thus do not plot them here. It should be noted that, although electron density profiles derived from ionograms may be reasonably extrapolated to altitudes above h_mF_2, the profiles above h_mF_2 do not represent their actual behaviors. During the sunrise enhancement, some features exhibited in the ionogram-derived profiles on 12 May 2004, such as the lifted h_mF_2, decreased f_oF_2, and distorted profiles, are similar to those from the simulations.

As shown in Figure 6, during the sunrise enhancement, the electron density below h_mF_2 is curtailed before 06:00 LT on 12 May. The bottomside profile distinctly increases in magnitude from 06:00 to 06:30 LT on 12 May. Meanwhile, the peak height recorded with the DPS rapidly reduces in magnitude. However, the vertical drift is upward at this period and should cause the plasma upward to make the bottomside electron density reduced and peak height lifted. Thus, the h_mF_2 observed by ionogram after 06:00 LT is new produced in the lower heights due to the drastically photochemical process instead of dropping of the lifted layer. Thereby, the lifted layer may be still existed at higher altitudes. The ionograms recorded by the Jicamarca DPS have a time resolution of 15 min. The interval of 15 min may make a condition that, when the ionograms are recorded by the ionosonde, the peak density of the lifted F_3 layer is lower than that of the new F_2 layer due to the strong photochemical process after sunrise. This may lead to fail to detect the F_3 layer in the ionograms.

Our simulations also suggest that a foF_3 higher than new f_oF_2 only lasts for a short time. Thus, the F_3 layer during the sunrise enhancement may be easy to be missed by using the ionosonde measurements with a time resolution of 15 min. In future study, it is worthy and possible to combine space-based observations with ISR measurements to further validate the relationship between the F_3 layers and the sunrise enhancement of the vertical drifts.

5. Summary

In this study, we report two cases of the sunrise enhancement in the *F* region vertical drift measured by the ISR over Jicamarca on 12 May and 10 June 2004. Under low solar activity and geomagnetic quiet times, the vertical drifts from the ISR observations can also enhance near sunrise in a way similar to the PRE near sunset. The Jicamarca ISR is regarded as the most powerful instrument to measure the equatorial ionospheric *F* region vertical plasma drifts. Thus, the two cases from the ISR measurements further provide evidence for the existence of sunrise enhancements in equatorial vertical drifts.

The effects of the sunrise enhancement on the ionosphere are, for the first time, investigated by using the ionograms from a Digisonde Portable Sounder at Jicamarca and conducting the Theoretical Ionospheric Model of the Earth in Institute of Geology and Geophysics, Chinese Academy of Sciences. In the DPS observations, the sunrise enhancement drift causes to lift the h_mF_2 significantly, and F_2 layer peak density and bottomside electron density tend to decrease compared to the days without sunrise enhancement drifts. The simulations from the TIME-IGGCAS show that, owing to the effect of the sunrise enhancement, the equatorial ionosphere is distinctly lifted, and the electron density profiles are distorted distinctly. What is more, the simulations tell the possible existence of the F_3 layer in the equatorial *F* region during the sunrise enhancements, while the normal F_2 layer develops at lower altitudes by the usual photochemical and dynamical processes.

Acknowledgments
The vertical drift data of the incoherent scatter radar are available from the web (jro.igp.gob.pe/madrigal/). We are grateful to B.W. Reinisch of the Center for Atmospheric Research, University of Massachusetts Lowell, for providing the ionogram data of DIDBase. The IMF *Bz* data are from the OMNI data set, which can be obtained from the GSFC/SPDF OMNIWeb interface (http://omniweb.gsfc.nasa.gov). The *Ap* and $F_{10.7}$ indices are obtained from the National Geophysical Data Center (http://spidr.ngdc.noaa.gov/spidr/). This research is supported by National Natural Science Foundation of China (41231065 and 41321003), National Key Basic Research Program of China (2012CB825604), and the Chinese Academy of Sciences project (KZZD-EW-01-3).

References

Abdu, M. A., et al. (2008), Abnormal evening vertical plasma drift and effects on ESF and EIA over Brazil-South Atlantic sector during the 30 October 2003 superstorm, *J. Geophys. Res.*, *113*, A07313, doi:10.1029/2007JA012844.

Adebesin, B. O., J. O. Adeniyi, I. A. Adimula, and B. W. Reinisch (2013), Low latitude nighttime ionospheric vertical E × B drifts at African region, *Adv. Space Res.*, *52*(12), 2226–2237, doi:10.1016/j.asr.2013.09.033.

Aggson, T. L., F. A. Herrero, J. A. Johnson, R. F. Pfaff, H. Laakso, N. C. Maynard, and J. J. Moses (1995), Satellite observations of zonal electric fields near sunrise in the equatorial ionosphere, *J. Atmos. Sol. Terr. Phys.*, *57*, 19–24, doi:10.1016/0021-9169(93)E0013-Y.

Balan, N., and G. J. Bailey (1995), Equatorial plasma fountain and its effects: Possibility of an additional layer, *J. Geophys. Res.*, *100*, 21,421–21,432, doi:10.1029/95JA01555.

Balan, N., G. J. Bailey, M. A. Abdu, K. I. Oyama, P. G. Richards, J. Macdougall, and I. S. Batista (1997), Equatorial plasma fountain and its effects over three locations: Evidence for an additional layer, the F_3 layer, *J. Geophys. Res.*, *102*, 2047–2056, doi:10.1029/95JA02639.

Balan, N., I. S. Batista, M. A. Abdu, J. MacDougall, and G. J. Bailey (1998), Physical mechanism and statistics of occurrence of an additional layer in the equatorial ionosphere, *J. Geophys. Res.*, *103*, 29,169–29,181, doi:10.1029/98JA02823.

Balan, N., I. S. Batista, M. A. Abdu, G. J. Bailey, S. Watanabe, J. MacDougall, and J. H. A. Sobral (2000), Variability of an additional layer in the equatorial ionosphere over Fortaleza, *J. Geophys. Res.*, *105*, 10,603–10,613, doi:10.1029/1999JA000020.

Basu, B., J. M. Retterer, O. de La Beaujardière, C. E. Valladares, and E. Kudeki (2004), Theoretical relationship between maximum value of the post-sunset drift velocity and peak-to-valley ratio of anomaly TEC, *Geophys. Res. Lett.*, *31*, L03807, doi:10.1029/2003GL018725.

Basu, S., S. Basu, J. Huba, J. Krall, S. E. McDonald, J. J. Makela, E. S. Miller, S. Ray, and K. Groves (2009), Day-to-day variability of the equatorial ionization anomaly and scintillations at dusk observed by GUVI and modeling by SAMI3, *J. Geophys. Res.*, *114*, A04302, doi:10.1029/2008JA013899.

Bittencourt, J. A., and M. A. Abdu (1981), A theoretical comparison between apparent and real vertical ionization drift velocities in the equatorial *F* region, *J. Geophys. Res.*, *86*, 2451–2454, doi:10.1029/JA086iA04p02451.

Fejer, B. G., E. R. de Paula, S. A. González, and R. F. Woodman (1991), Average vertical and zonal *F* region plasma drifts over Jicamarca, *J. Geophys. Res.*, *96*, 13,901–13,906, doi:10.1029/91JA01171.

Fejer, B. G., L. Scherliess, and E. R. de Paula (1999), Effects of the vertical plasma drift velocity on the generation and evolution of equatorial spread F, *J. Geophys. Res.*, *104*, 19,859–19,869, doi:10.1029/1999JA900271.

Fesen, C. G., G. Crowley, R. G. Roble, A. D. Richmond, and B. G. Fejer (2000), Simulation of the pre-reversal enhancement in the low latitude vertical in drifts, *Geophys. Res. Lett.*, *27*, 1851–1854, doi:10.1029/2000GL000061.

Hanson, W. B., and R. J. Moffett (1966), Ionization transport effects in the equatorial *F* region, *J. Geophys. Res.*, *71*, 5559–5572, doi:10.1029/JZ071i023p05559.

Hedin, A. E., et al. (1996), Empirical wind model for the upper, middle and lower atmosphere, *J. Atmos. Terr. Phys.*, *58*, 1421–1447, doi:10.1016/0021-9169(95)00122-0.

Huang, X., and B. W. Reinisch (2001), Vertical electron content from ionograms in real time, *Radio Sci.*, *36*, 335–342, doi:10.1029/1999RS002409.

Kelley, M. C., F. S. Rodrigues, R. F. Pfaff, and J. Klenzing (2014), Observations of the generation of eastward equatorial electric fields near dawn, *Ann. Geophys.*, *32*, 1169–1175, doi:10.5194/angeo-32-1169-2014.

Kil, H., S.-J. Oh, L. J. Paxton, and T.-W. Fang (2009), High-resolution vertical E × B drift model derived from ROCSAT-1 data, *J. Geophys. Res.*, *114*, A10314, doi:10.1029/2009JA014324.

Klimenko, M. V., V. V. Klimenko, and A. T. Karpachev (2012), Formation mechanism of additional layers above regular F_2 layer in the near-equatorial ionosphere during quiet period, *J. Atmos. Sol. Terr. Phys.*, *90-91*, 179–185, doi:10.1016/j.jastp.2012.02.011.

Kudeki, E., S. Bhattacharyya, and R. F. Woodman (1999), A new approach in incoherent scatter *F* region E × B drift measurements at Jicamarca, *J. Geophys. Res.*, *104*, 28,145–28,162, doi:10.1029/1998JA900110.

Mannucci, A. J., B. T. Tsurutani, B. A. Iijima, A. Komjathy, A. Saito, W. D. Gonzalez, F. L. Guarnieri, J. U. Kozyra, and R. Skoug (2005), Dayside global ionospheric response to the major interplanetary events of October 29–30, 2003 Halloween storms, *Geophys. Res. Lett.*, *32*, L12S02, doi:10.1029/2004GL021467.

Millward, G. H. (1993), A global model of the Earth's thermosphere, ionosphere and plasmasphere: Theoretical studies of the response to enhanced high-latitude convection, PhD dissertation, Univ. of Sheffield, U. K.

Picone, J. M., A. E. Hedin, D. P. Drob, and A. C. Aikin (2002), NRLMSISE-00 empirical model of the atmosphere: Statistical comparisons and scientific issues, *J. Geophys. Res.*, *107*(A12), 1468, doi:10.1029/2002JA009430.

Scherliess, L., and B. G. Fejer (1999), Radar and satellite global equatorial *F* region vertical plasma drift model, *J. Geophys. Res.*, *104*, 6829–6842, doi:10.1029/1999JA900025.

Sen, H. Y. (1949), Stratification of the F_2-layer of the ionosphere over Singapore, *J. Geophys. Res.*, *54*, 363–366, doi:10.1029/JZ054i004p00363.

Woodman, R. F. (1970), Vertical drift velocities and east-west electric fields at the magnetic equator, *J. Geophys. Res.*, *75*, 6249–6259, doi:10.1029/JA075i031p06249.

Yue, X., W. Wan, L. Liu, H. Le, Y. Chen, and T. Yu (2008), Development of a middle and low latitude theoretical ionospheric model and an observation system data assimilation experiment, *Chin. Sci. Bull.*, *53*(1), 94–101, doi:10.1007/s11434-007-0462-z.

Zhang, R., L. Liu, Y. Chen, and H. Le (2015), The dawn enhancement of the equatorial ionospheric vertical plasma drift, *J. Geophys. Res. Space Physics*, *120*, 10,688–10,697, doi:10.1002/2015JA021972.

Zhao, B., W. Wan, B. Reinisch, X. Yue, H. Le, J. Liu, and B. Xiong (2011a), Features of the F_3 layer in the low-latitude ionosphere at sunset, *J. Geophys. Res.*, *116*, A01313, doi:10.1029/2010JA016111.

Zhao, B., W. Wan, X. Yue, L. Liu, Z. Ren, M. He, and J. Liu (2011b), Global characteristics of occurrence of an additional layer in the ionosphere observed by COSMIC/FORMOSAT-3, *Geophys. Res. Lett.*, *38*, L02101, doi:10.1029/2010GL045744.